Appl Nanosci (2014) 4:989–996
DOI 10.1007/s13204-013-0280-3

ORIGINAL ARTICLE

Stability and electronic properties of isomers of B/N co-doped graphene

Pooja Rani · V. K. Jindal

Received: 26 September 2013 / Accepted: 30 October 2013 / Published online: 15 November 2013

Abstract We study and compare some of the possible isomers of BN co-doped graphene on the basis of their composition and electronic properties. The effect of doping has been studied theoretically by substituting the C atoms of graphene with an equal amount of B/N with their concentration varying from 4 % (2 atoms of the dopant in 50 host atoms) to 24 % and choosing different doping sites for each concentration. We made use of VASP (Vienna Ab-initio Simulation Package) software based on density functional theory to perform all calculations. While the resulting geometries do not show much of distortion on doping, the electronic properties show a transition from semimetal to semiconductor with increasing number of dopants as in the case of individual B and N doping. The study shows that the BN doping introduces the band gap at the Fermi level unlike individual B and N doping which causes the shifting of Fermi level. High value of the cohesive energy indicates the stability of the resulting heterostructures. Isomers formed by choosing different doping sites differ significantly in relative stability and band gap introduced and these aspects, to a great extent, depend upon position of B and N atoms in the heterostructure.

Keywords Graphene · Isomer · Doping · Stability · Band gap · Density functional theory

P. Rani (✉) · V. K. Jindal
Department of Physics, Panjab University, Chandigarh 160014, India
e-mail: pgoyal0510@gmail.com

Introduction

Graphene is the name given to a single layer of sp^2 bonded carbon atoms arranged in a honeycomb pattern. It is a thermodynamically stable two-dimensional material, in which the valence and conduction bands touch at the so-called Dirac point and so is always referred as a semi-metal or zero-gap semiconductor. Since its successful fabrication in 2004 by micromechanical cleavage of graphite at the University of Manchester, UK, by the group of Geim (Novoselov et al. 2004), it has attracted great interest due to its fascinating properties and potential applications. Graphene has unique physical properties (Novoselov et al. 2004, 2005; Geim and Novoselov 2007; Castro Neto et al. 2009) like massless relativistic fermions that satisfy the Dirac equation, high electrical conductivity (even greater than silver) at room temperature, anomalous quantum Hall effect, optical transparency (Nair et al. 2008), finite conductivity even at zero charge carrier concentration and ballistic transport which originate from its hexagonal honeycomb lattice structure and make it a promising material for application in future nanoelectronics (Novoselov et al. 2006; Yang et al. 2010; Huang et al. 2007; Morozov et al. 2008), sensors (Romero et al. 2009) and optoelectronic applications (Bonaccorso et al. 2010). The linear dispersion curve at the Dirac point gives rise to exciting elementary electronic properties.

The special character of its charge carriers comes from the intersection of the π/π^* electronic bands occurring at the corners of its hexagonal Brillouin zone (Fig. 1). *P6/mmm* symmetry of the space group results in a band degeneracy at the Dirac points (K and K') in the hexagonal Brillouin zone (BZ) leading to zero band gap. This absence of a sizable band gap in graphene sets limitations on its practical applications. So it is of crucial importance to find

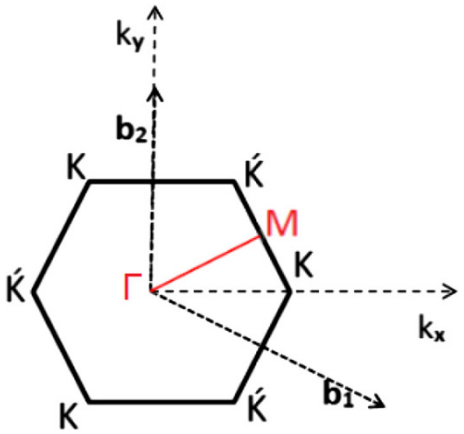

Fig. 1 Hexagonal Brillouin zone of graphene

methods to effectively tune the band gap of graphene for applications in nanoelectronics and optoelectronics.

A great amount of effort has been devoted to open a tunable band gap in graphene and different methods have been proposed: chemical functionalization (Wang et al. 2009; Bekyarova et al. 2009; Sofo et al. 2007; Zanella et al. 2008; Choi et al. 2009), doping with heteroatoms (Denis 2010; Dai et al. 2009), using electric fields (Avetisyan et al. 2009; Mak et al. 2009) and depositing graphene on substrates like SiO_2, SiC (Shemella and Nayak 2009; Peng and Ahuja 2008).

Doping with heteroatoms, especially B and N is a widely used technique to modulate the electronic properties (Panchakarla et al. 2009; Wu et al. 2010; Faccio 2010; Tang et al. 2012; Gebhardt et al. 2013) in graphene. B and N are neighboring elements of carbon in the periodic table and have nearly same size and mass that of carbon.

It has been shown by Wu et al. (2010) and in (Rani and Jindal 2013), that doping with B or N individually is an efficient method to open the band gap around the Dirac point, but it introduces the gap below or above the Fermi level. Further, as compared to B–B or N–N bond lengths, B–N bond length is comparable to C–C bond length, which makes the combination of B–N as a better choice to replace a C–C bond without causing much alteration of 2-D lattice. However, introduction of BN in graphene breaks the symmetry of graphene unit cell (Bhandary and Sanyal 2012), which can result in the opening up of a band gap in graphene and can be exploited for band gap-related applications.

It has been pointed out by Deng et al. (2011) that in case of BN co-doping, the gap is introduced at the Fermi level due to combination of pull–push of boron and nitrogen. Fan et al. (2012) have investigated the effect of concentration by varying the number of host atoms, and Manna and Pati (2011) have shown that the patching of graphene and h-BN sheet with semiconducting and/or insulating BxNy(Cz) nanodomains of various geometrical shapes and sizes (h-BN sheet) can significantly change the electronic and magnetic properties. The comparison of stability and band gap of the isomers of B–C–N composites have been studied by Bhandary and Sanyal (2012). However, the detailed analysis of varying concentration (changing the number of BN dopants) and position of B–N pairs and hence the interaction between them and their effect on the stability and band gap of resulting structures is yet to be done.

Fig. 2 Optimized geometries and band structures of different isomers in increasing order of dopant concentration [4 % (**A**), 8 % (**B**), 12 % (**C**), 16 % (**D**), 20 % (**E**) and 24 % (**F**)], respectively. In isomer a, B and N are at ortho position, in isomer b same type of dopants (B or N) are placed at adjacent positions, in isomer c, B and N are at para position (isomer c) and in isomer d, BN pair is at ortho position but distance between two BN pairs is large. Due to higher doping concentration the category (d) cannot be possible in 2 (**E**) and 2 (**F**)

Therefore, in this paper we find it worthwhile to study the structural stability and the effect on band opening by incorporation of BN with different concentrations by increasing the number of BN dopants and also taking into account different possible doping sites.

Models and computational parameters

Structure minimization and electronic structure calculations have been performed using the VASP (Vienna Ab-initio Simulation Package) (Kresse and Furthmüller 1996; Kresse and Joubert 1999) code which uses plane waves as basis set. The approach is based on an iterative solution of the Kohn–Sham equation (Kohn and Sham 1965) of the density functional theory (DFT). That DFT methods underestimate the band gap of materials, is well known. However, standard DFT methods correctly describe the electronic properties of both graphene and BN (Liu et al. 2003). Therefore, DFT can be fairly used to describe electronic properties of graphene doped by BN, though underestimation of the band gap is possible.

In our calculations, core electrons are replaced by the projector-augmented wave pseudo-potentials and the Perdew–Wang (PW91) (Blöchl 1994) exchange–correlation (XC) functional of the generalized gradient approximation (GGA) is adopted. The plane-wave cutoff energy was set to 450 eV. The calculations of lattice constants and the atomic coordinates at different doping concentrations are made by the minimization of the total energy. A graphene sheet model of 5 × 5 supercell consisting of 50 atoms have been considered for the calculations. The vertical separation between the two sheets has been fixet at 15 Å to avoid the interplanar interactions. We have doped equal amount of B and N concentration thus generating equal number of C–B and C–N bonds. This results in practically identical

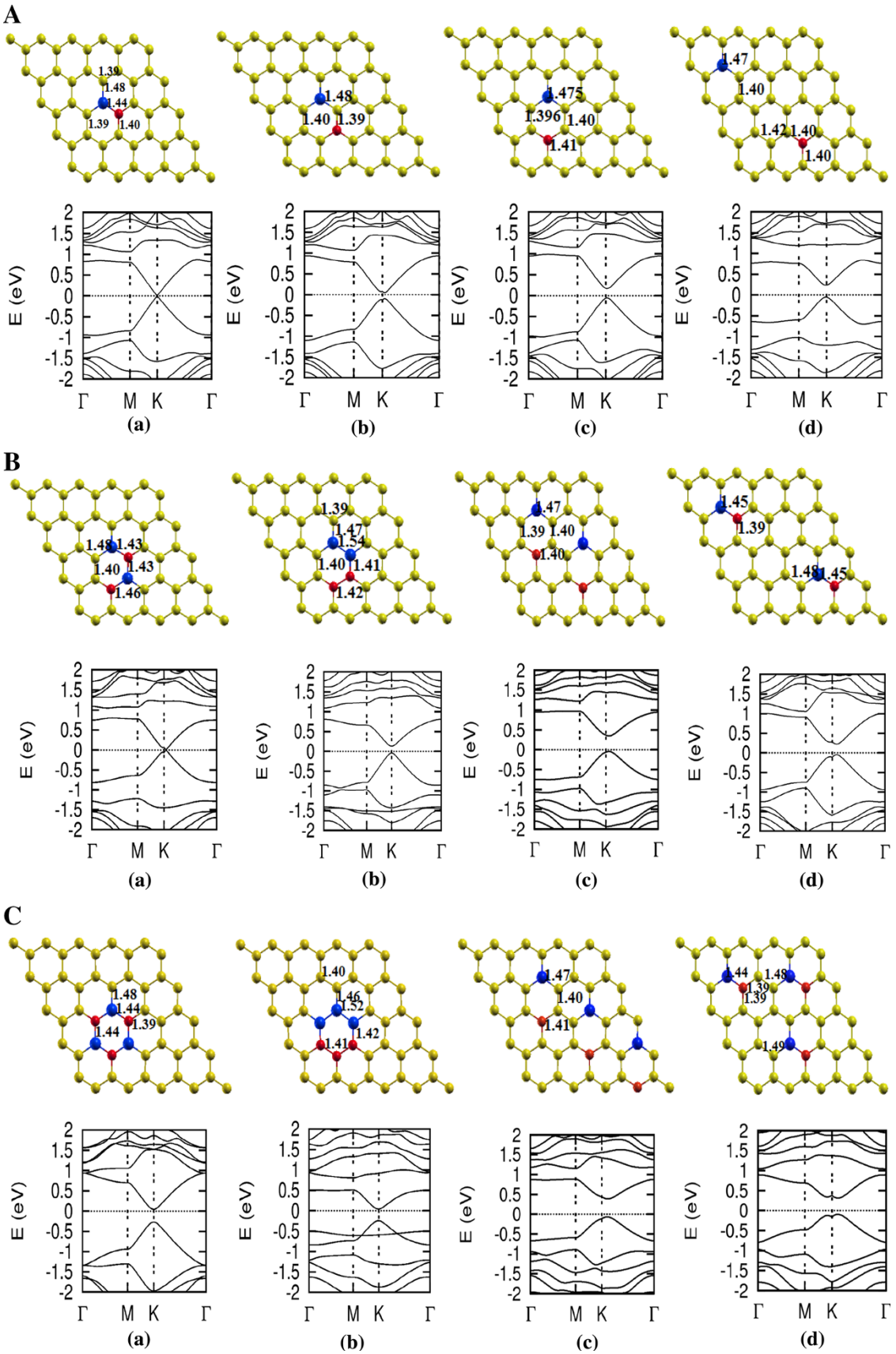
A
1.39
1.48
1.44
1.39
1.40
1.48
1.40
1.39
1.475
1.396
1.40
1.41
1.47
1.40
1.42
1.40
1.40
E (eV)
Γ M K Γ
(a)
(b)
(c)
(d)
B
1.48
1.43
1.40
1.43
1.46
1.39
1.47
1.54
1.40
1.41
1.42
1.47
1.39
1.40
1.40
1.45
1.39
1.48
1.45
C
1.48
1.44
1.39
1.44
1.40
1.46
1.52
1.42
1.41
1.47
1.40
1.41
1.44
1.48
1.39
1.39
1.49

average atom–atom distance. The Monkhorst–Pack scheme is used for sampling the Brillouin zone. In the calculations, the structures are fully relaxed with a Gamma-centered 7 × 7 × 1 k-mesh. During all calculation processes, the partial occupancies were treated using the tetrahedron methodology with Blöchl corrections (Blöchl et al. 1994). For band structure calculation, partial occupancies for each wavefunction were determined using the Gaussian smearing method with a broadning of 0.01 eV. For geometry optimizations, all the internal coordinates were relaxed until the Hellmann–Feynman forces were <0.008 eV/Å. In order to give a numerical account of the stability of the doped systems, cohesive energy has been calculated using the following expression:

$$^{*}E_{\mathrm{coh}}=[E_{\mathrm{tot}}-n_iE_i]/n(i = \mathrm{C, B, N}),$$

where E_{coh} is the cohesive energy per atom of BN-doped configuration and E_{tot} and E_i represent total energies of a structure and of individual elements present within the same supercell, respectively. n_i is the number of ith species present in the configuration, while n is the total number of atoms present in a supercell ($n = 50$). A pure graphene sheet was optimized and its bond length and band structure (Geim and Novoselov 2007) are in accordance with literature which confirms the reliability of the simulation method used.

Results and discussion

We carry out our calculations with different concentrations of BN doping (4, 8, 12, 16, 20 and 24 %) in graphene and also take into account different sites of doping for the same concentration. Although we analyze several possible isomers for different concentrations of dopants, for the sake of brevity, we present here only a few isomers with the configurations of mainly four doping sites, i.e. when B and N are at ortho position (isomer a), when same type of dopants (B or N) are at adjacent positions (isomer b), para position (isomer c) and when BN pair is at ortho position but distance between two BN pairs is large (d). The structures of different isomers corresponding to different dopant concentrations are given in Fig 2.

Comparative stability of the isomers

The replacement of two carbon atoms with B–N introduces several interesting features. First, there is very small difference between B–N bond (1.45 Å) and C–C bond length (1.42 Å), but C–B (1.49 Å) bond is 15 % longer than C–N (1.35 Å) bond. So, this will cause distortion in the doped structures, which is going to lower its stability than pure graphene. Second, as mentioned earlier, this will break sublattice symmetry in graphene and bring a significant change in electronic properties. Having these points in mind, in this section we will discuss the stability for various isomers at different concentrations.

We observe that for the low doping concentrations the isomers are more or less energy equivalent, as in the case of 4 % doping concentration (Fig 2A). This is due to the fact that aromaticity and π-band formation of the C-ring do not change much as a whole, which makes those structures iso-energetic. But as the doping concentration goes on increasing, the energy difference becomes significant. This is due to increase in number of B–C, N–C, B–B and N–N bonds and the mismatch leads to strain in the structure. So the structures with more number of these bonds are significantly less stable than other isomers with same doping concentration [see category (c) of Fig 2B–F]. Also the stability for the same doping concentration is greater as compared to the separate B or N doping. This may be due to the equal number of C–B and C–N bonds.

The second observation is that the isomers in which BN is placed as a pair (ortho positions), have considerably larger cohesive energy and hence more stable than their counterparts (para positions) in which B and N are apart. This is due to more stable B–N bond than B–C or N–C bond. When the bond energies are numerically taken into account, the ordering of the bonds is the following (Bhandary and Sanyal 2012; Nozaki and Itoh 1996):

$$\begin{aligned}&\mathrm{B-N\ (4.00\ eV)\ > C-C\ (3.71\ eV)\ >}\\&\mathit{N}\mathrm{-C\ (2.83\ eV)\ > B-C\ (2.59\ eV)\ >}\\&\mathit{B}\mathrm{-B\ (2.32\ eV)\ > N-N\ (2.11\ eV)}\end{aligned}$$

So in a way the isomers having more number of C–C or B–N bonds will have more stability over the others.

Thus there is apparent competition between structural stress and chemical bond strength that can be described by calculating the internal energies of the different geometries which are given in Table 1.

Another important aspect is the charge transfer. N is the most electronegative and B is the least one among the three atoms. In case of single BN pair-doped graphene the net charge on N is −1.54 e and +1.82 e on B. This introduces an ionic character in the bond formation. So presence of a B–B or N–N bond makes the structure unstable due to electrostatic repulsion. If the positive and negative charges are situated in an alternative manner, as in case of B–N, binding energy is increased providing stability to the structure [see category (a) of the isomers]. The results show that the B and N binding together is energetically more favorable than being separate in the hexagonal network.

The analysis of structural properties shows the shrinkage of C–C bond lengths which are just adjacent to boron atoms [see isomers (b) in Fig 2] dopants. This possibly results from longer C–B bond lengths because of large

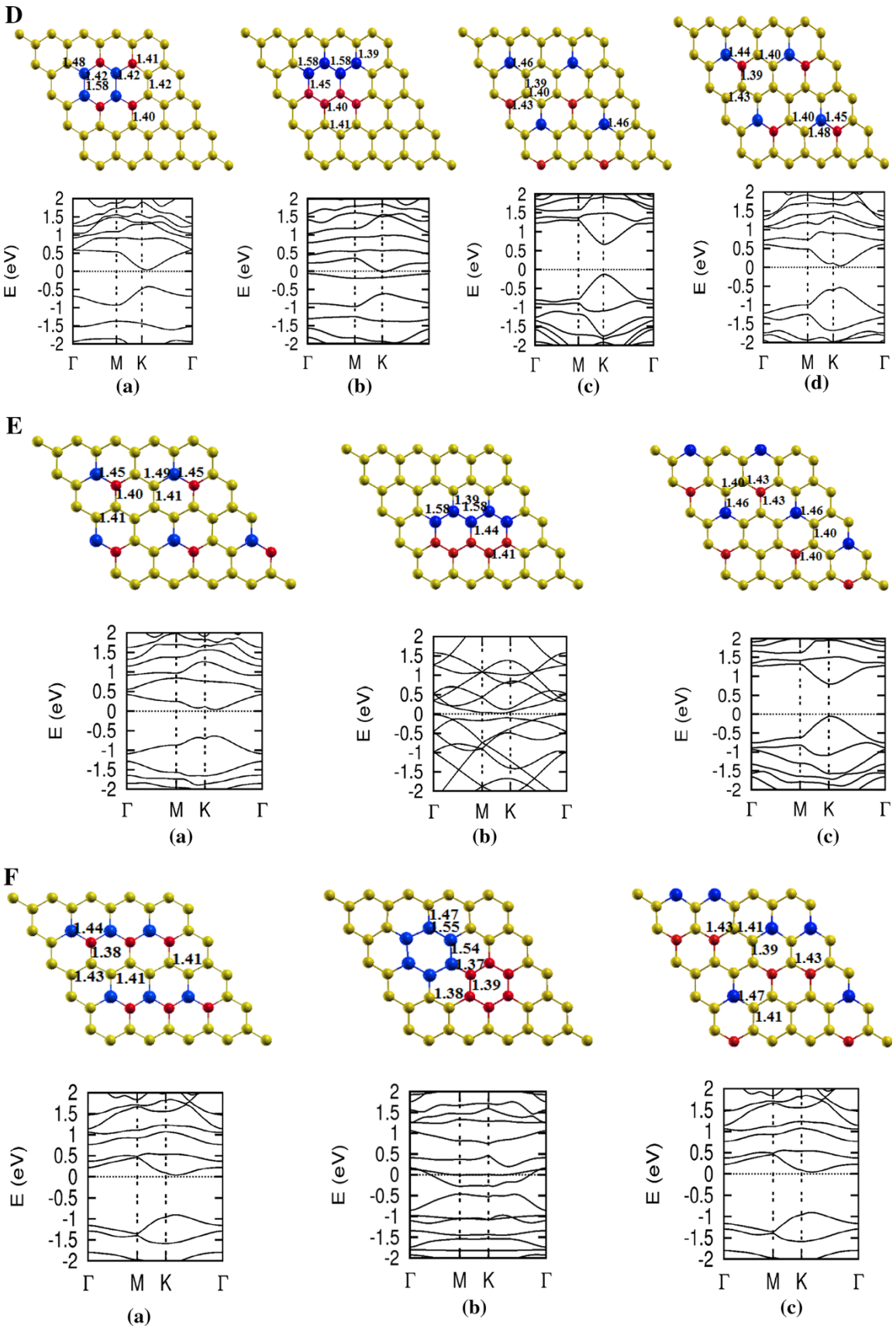

Fig. 2 continued

Table 1 Cohesive energy and band gap for increasing doping concentration and various possible configurations a, b, c, d as described in Fig. 2

BN concentration (%)	Configuration (as shown in Fig. 3)	E^{*}_{coh} (eV/atom)	Band gap (eV)
4	a	−9.13	0.20
	b	−9.11	0.00
	c	−9.11	0.25
	d	−9.10	0.28
8	a	−9.09	0.09
	b	−9.04	0.18
	c	−9.06	0.40
	d	−9.10	0.43
12	a	−9.04	0.31
	b	−8.93	0.28
	c	−8.98	0.56
	d	−9.02	0.58
16	a	−8.98	0.56
	b	−8.80	0.20
	c	−8.95	0.73
	d	−8.87	0.79
20	a	−8.93	0.83
	b	−8.67	0.20
	c	−8.82	0.85
24	a	−8.94	1.06
	b	−8.39	0.48
	c	−8.71	1.08

covalent radius of B than C and preservation of the structure. This also results in large strain in the lattice when the dopants are placed at adjacent positions. The data regarding changes in bond lengths are presented in the structural part of the figures presented in Fig 2.

Electronic properties

The redistribution of surface charge which breaks the local symmetry of graphene is the main reason of band gap opening of graphene on BN doping, which leads to the separation of the valence band and conduction band of graphene at the Dirac point. Since B doping leads to band gap opening below the Fermi level and N doping, above the Fermi level, the counterbalance of both creates a gap at the Fermi level. In addition, the coulomb dipole from BN molecule may also be important to the breaking of symmetry of graphene structure and thus to the band gap opening.

The electronic structure analysis shows that band gap in general increases with increase in concentration of doping. The values of the band gap corresponding to different doping concentrations and isomers are given in Table 1. We give in Fig. 3 a plot of this variation of band gap with % concentration of dopants for the largest band gap for each concentration. We see that the variation of band gap with dopant concentration is almost linear.

As shown by Bhandary and Sanyal (2012), the relative positions of B and N around an all C hexagon is an important factor that determines the electronic properties of the doped isomer. We observe that the band gap is more in the structure in which B and N are at para-positions than the isomer in which they are at ortho positions. This tells us that the interaction between B/N pair also plays an important role in the formation of the band gap.

The width of band gap goes on increasing with the increase in distance between B and N atoms, as shown in Fig. 2 [category (c)], which can be explained by the sum of the effects of Boron and Nitrogen doping into graphene, whereas single Boron or Nitrogen atom doping will break the π bond with inducing a gap in the valence or conduction band only. This also explains the higher band gap as compared to the individual B and N doping. Also when distance between two BN pairs increases, the ortho-para aspect has no effect, i.e. the isomers with ortho and para arrangement of BN pairs have almost same band gap because ortho-para effect has more pronounced effect in case of single hexagon.

From the Fig. 2 it can be observed that for [configuration (b)] corresponding to different concentrations, containing B–B and N–N at adjoint positions, band structure is highly deformed and linear dispersion relation at the Dirac point is also affected. This can be explained by the fact that linear dispersion in graphene is due to its crystal symmetry. So when the dopants are placed at adjacent positions as in isomers. (a), the symmetry is highly distorted which results into deformation of band structure. Also the band gap is minimum in this case.

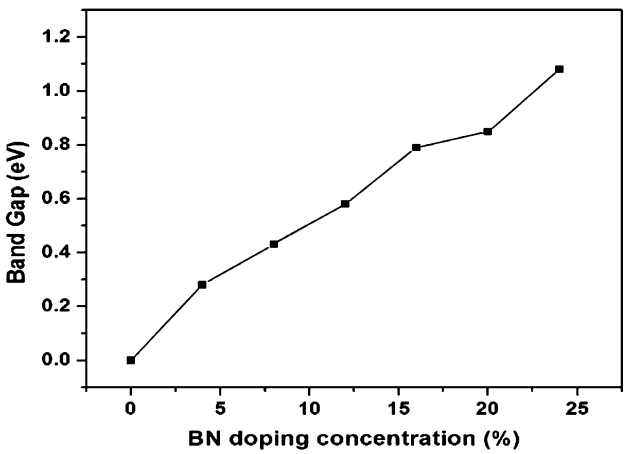

Fig. 3 Variation of band gap with increasing concentration of BN dopants. The *plot* is drawn for the maximum value of band gap for each concentration

Conclusion

Ab-initio calculations were performed to analyze the geometry and electronic structure of isomers of BN-doped graphene sheet. We observe transition of graphene from semimetal to semiconductor with increasing number of dopants. It has been observed that isomers formed by choosing various doping sites differ in the stability, bond length and band gap introduced, depending upon the positioning of the dopant atoms. Thus, through our detailed analysis, we suggest a theoretical approach to design heterographenes with different amount and composition of either B or N doping (Rani and Jindal 2013) or codoping of both (BN). Both mechanisms result in tuning of band gap in a wide range, for device applications. While B or N doping results in band gap at Dirac point with shifting of Fermi Level, BN codoping creates the gap at Fermi level, thus being more efficient. Due to their tunable band structure properties, the resulting materials can be used in applications in various sectors, e.g., nano electronics, gas sensing and hydrogen storage. BN-doped graphene can act as a good electrocatalyst for oxygen reduction reaction (ORR) due to high electron density present on the N atom in BCN heterostructure. Some experimental study in this direction was performed recently by Shuangyin et al. to prepare BN co-doped graphene with tunable composition which has superior electrocatalytic activity over commercial Pt/C electrocatalysts for the oxygen (Wang et al. 2012). The study supports our results and motivates to do further work in this direction.

Acknowledgments We express our gratitude to VASP team for providing the code, the HPC facilities at IUAC (New Delhi) and the departmental computing facilities at Department of Physics, PU, Chandigarh. PR gratefully acknowledges financial support from UGC. VKJ acknowledges support from CSIR as Emeritus Scientist.

References

Avetisyan AA, Partoens B, Peeters FM (2009) Electric field tuning of the band gap in graphene multilayers. Phys Rev B 79:035421

Bekyarova E, Itkis ME, Ramesh P, Berger C, Sprinkle M, De Heer WA, Haddon RC (2009) Chemical modification of epitaxial graphene: spontaneous grafting of aryl groups. J Am Chem Soc 131:1336–1337

Bhandary S, Sanyal B (2012) Graphene-boron nitride composite: a material with advanced functionalities. In: Ning Hu (ed) Composites and their properties. InTech, Rijeka, pp 1–14

Blöchl PE (1994) Projector augmented-wave method. Phys Rev B 50:17953

Blöchl PE, Jepsend O, Andersen OK (1994) Improved tetrahedron method for Brillouin-zone integrations. Phys Rev B 49: 16223–16233

Bonaccorso F, Sun Z, Hasan T, Ferrari AC (2010) Graphene photonics and optoelectronics. Nat Photonics 4:611–622

Castro Neto AH, Guinea F, Peres NMR, Novoselov KS, Geim AK (2009) The electronic properties of graphene. Rev Mod Phys 81:109–162

Choi J, Kim K-J, Kim B, Lee H, Kim S (2009) Covalent functionalization of epitaxial graphene by azidotrimethylsilane. J Phys Chem C Lett 113:9433–9435

Dai J, Yuan J, Giannozzi P (2009) Gas adsorption on graphene doped with B, N, AL, S: a theoretical study. Appl Phys Lett 95:232105

Deng X, Wu Y, Dai J, Kang D, Zhang D (2011) Electronic structure tuning and band gap opening of graphene by hole/electron codoping. Phys Lett A 375:3890–3894

Denis PA (2010) Band gap opening of monolayer and bilayer graphene doped with aluminium, silicon, phosphorus and sulfur. Chem Phys Lett 492:251–257

Faccio R, Fernández-Werner L, Pardo H, Goyenola C, Ventura ON, Mombrú AW (2010) Electronic and structural distortions in graphene induced by carbon vacancies and boron doping. J Phys Chem C 114:18961–18971

Fan X, Shen Z, Liu AQ, Kuo JL (2012) Band gap opening of graphene by doping small boron nitride domains. Nanoscale 4:2157–2165

Gebhardt J, Koch RJ, Zhao W, Hofert O, Gotterbarm K, Mammadov S, Papp C, Gorling A, Steinruck H-P, Seyller Th (2013) Growth and electronic structure of boron-doped graphene. Phys Rev B 87:155437

Geim AK, Novoselov KS (2007) The rise of graphene. Nat Mater 6:183–191

Huang B, Yan QM, Zhou G, Wu J, Gu BL, Duan WH, Liu F (2007) Appl Phys Lett 91:253122

Kohn W, Sham LJ (1965) Self-consistent equations including exchange and correlation effects. Phys Rev A 140:1133–1138

Kresse G, Furthmüller J (1996) Efficient iterative schemes for *ab - initio* total energy calculations using a plane-wave basis set. Phys Rev B 54:11169–11186

Kresse G, Joubert D (1999) From ultrasoft pseudopotentials to the projector augmented-wave method. Phys Rev B 59:1758–1775

Liu Lei, Feng YP, Shen ZX (2003) Structural and electronic properties of h-BN. Phys Rev B 68:104102

Mak KF, Lui CH, Shan J, Heinz TF (2009) Observation of an electric-field-induced band gap in bilayer graphene by infrared spectroscopy. Phys Rev Lett 102:256405

Manna AK, Pati SK (2011) Tunable electronic and magnetic properties in BxNyCz Na nohybrids: effect of domain segregation. J Phys Chem C 115:10842–10850

Morozov SV, Novoselov KS, Katsnelson MI, Schedin F, Elias DC, Jaszczak JA, Geim AK (2008) Giant intrinsic carrier mobilities in graphene and its bilayer. Phys Rev Lett 100:016602

Nair RR, Blake P, Grigorenko AN, Novoselov KS, Booth TJ, Stauber T, Peres NMR, Geim AK (2008) Fine structure constant defines visual transparency of graphene. Science 320:1308

Novoselov KS, Geim AK, Morozov SV, Jiang D, Zhang Y, Dubonos SV, Grigorieva IV, Firsov AA (2004) Electric field effect in atomically thin carbon films. Science 306:666–669

Novoselov KS, Geim AK, Morozov SV, Jiang D, Katesnelson MI, Grigoreva V, Dubonos SV, Firsov AA (2005) Two-dimensional gas of massless Dirac fermions in graphene. Nature (London) 438:197–200

Novoselov KS, McCann E, Morozov SV, Fal'ko VI, Katsnelson MI, Zeitler U, Jiang D, Schedin F, Geim AK (2006) Unconventional quantum Hall effect and Berry's phase of 2π in bilayer graphene. Nature Phys 2:177–180

Nozaki H, Itoh S (1996) Structural stability of BC_2N. J Phys Chem Solids 57:41–49

Panchakarla LS, Subrahmanyam KS, Saha, Achutharao Govindaraj SK, Rishnamurthy HR, Waghmare UV, Rao CNR (2009) Synthesis, structure, and properties of boron- and nitrogen-doped graphene. Adv Mat 21:4726–4730

Peng X, Ahuja R (2008) Symmetry breaking induced bandgap in epitaxial graphene layers on SiC. Nano Lett 8:4464–4468

Rani Pooja, Jindal VK (2013) Designing band gap of graphene by B and N dopant atoms. RSC Adv 3:802–812

Romero HE, Joshi P, Gupta AK, Gutierrez HR, Cole MW, Tadigadapa SA, Eklund PC (2009) Adsorption of ammonia on graphene. Nanotechnology 20:245501

Shemella P, Nayak SK (2009) Appl Phys Lett 94:032101

Sofo JO, Chaudhari AS, Barber GD (2007) Graphane: a two-dimensional hydrocarbon. Phys Rev B 75:153401

Tang YB, Yin LC, Yang Y, Bo XH, Cao YL, Wang HE, Zhang WJ, Bello I, Lee ST, Cheng HM, Lee CS (2012) Tunable band gaps and p-type transport properties of boron-doped graphenes by controllable ion doping using reactive microwave plasma. ACS Nano 6:1970–1978

Wang X, Li X, Yoon Y, Weber PK, Wang H, Guo J, Dai H (2009) N-doping of graphene through electrochemical reactions with ammonia. Science 324:768–771

Wang S, Zhang L, Xia Z, Roy A, Chang DW, Baek JB, Dai L (2012) BCN graphene as efficient metal-free electrocatalyst for the oxygen reduction reaction. Angew Chem 124:4285–4288

Wu M, Cao C, Jiang JZ (2010) Light non-metallic atom (B, N, O and F)-doped graphene: a first-principles study. Nanotechnology. 21:505202

Yang XB, Liu GX, Balandin AA, Mohanram K (2010) Triple-mode single-transistor graphene amplifier and its applications. ACS Nano 4:5532–5538

Zanella I, Guerini S, Fagan SB, Mendes J, Filho AG, Souza Filho (2008) Chemical doping-induced gap opening and spin polarization in graphene. Phys Rev B 77:073404